

## Conjugated Polymer/Molten Salt Blend Optimization

F. Habrard, T. Ouisse,\* and O. Stéphan

*Laboratoire de Spectrométrie Physique, Université Joseph Fourier, Grenoble 1 and CNRS (UMR C5588), 140, rue de la physique, BP87, 38402, Saint-Martin d'Hères Cedex, France**Received: June 13, 2006; In Final Form: July 3, 2006*

Light-emitting electrochemical cells with low current threshold can be realized through mixing conjugated polymers and molten salts. Current drive capability is proportional to the overall interface perimeter of the planar, discotic molten salt domains inserted into the polymer matrix. Electric force microscopy indicates that this interface perimeter exhibits a specific dependence on the molten salt content in the active layer, with a well-defined maximum. We show that this maximum corresponds to an optimal current drive.

## Introduction

Room temperature ionic liquids are currently studied in order to improve the properties of lithium secondary batteries (see, e.g., ref 1 and references therein). Recently we have shown that they can also be put to good use to improve the properties of organic light emitters.<sup>2–4</sup> Organic light-emitting diodes (OLED) are currently developed to produce low-cost, low power consuming displays, some of them being already incorporated into commercial products such as mobile phones. The use of polymer-based devices would allow one to further reduce production costs. Short wavelength light emitters based upon the use of conjugated polymers exhibit high energy barriers against electron injection, corresponding to high threshold voltages.<sup>3</sup> An effective way to lower this threshold consists of mixing an electrolyte with the conducting polymer to form light-emitting electrochemical cells (LECs).<sup>2–10</sup> Creation of electrolytic double layers at the electrode-active layer interface and bulk electrochemical doping result in threshold voltages of the order of the polymer band gap, even for electrode metals totally unsuited for conventional OLED operation.<sup>2–11</sup> A convenient way to fabricate LECs is to mix a molten salt and the conjugated polymer in the solution to be spin-coated for fabricating the active layer.<sup>2–4</sup> Device performance mainly depends on the blend morphology, so that improving the blend quality is a key factor.<sup>12</sup> In this letter, we show through combined atomic force microscope (AFM) and electrical measurements that for a given couple of ionic liquid and polymer, a well-defined optimum blend allows one to maximize the current drive capability. In a previous work, we presented an AFM study of the phase separation occurring in the blend,<sup>12</sup> which revealed that the active layer morphology takes the form of molten salt discs inserted in a polymer matrix. In this former report we established a definite correlation between the current drive capability and the length defined by the interface between the polymer and molten salt domains. Injection being enhanced in the polymer areas closest to the ionic domains, the current improves with an increase in the overall perimeter of the molten salt domains.<sup>12</sup>

\* To whom correspondence should be addressed. E-mail: ouisse@spectro.ujf-grenoble.fr. Fax: 33 4 76 63 54 95. Phone 33 4 76 51 47 71.

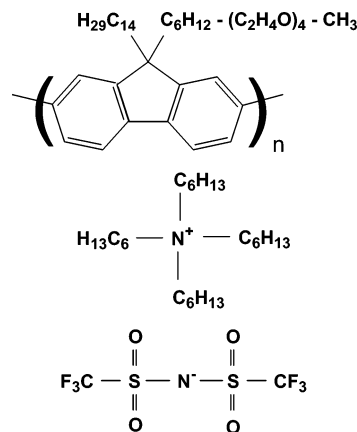


**Figure 1.** Chemical structure of the fluorene-based polymer functionalized with an alkyl chain and a PEO segment (top) and of the room-temperature molten salt (bottom).

Here we focus on a particular couple of polymer and salt, and vary the ratio between the molten salt and polymer contents. We acquired electric force microscopy (EFM) images from a large number of different blends. We find that the perimeter per unit area of the molten salt domains  $L_{SP}$  exhibits a well-defined maximum as a function of the overall salt content. Measurements carried out with LECs processed with various molten salt concentrations confirm that this maximum in  $L_{SP}$  does correspond to a maximum current drive capability.

**Sample and Device Fabrication.** We use a fluorene-based polymer functionalized with an alkyl chain and a poly(ethylene oxide) (PEO) segment as shown in Figure 1. The molten salt is tetra-hexyl-ammonium tri-fluoro-methyl-sulfonyl-imide (hereafter referred to as THA-TFSI, see Figure 1). Both the polymer and salt are synthesized in our laboratory. For more details on materials, see, e.g., ref 12. Incorporation of PEO segments favors polymer-salt mixing during the spin-coating process. The blend is characterized by the presence of numerous discotic salt domains uniformly distributed through the polymer layer. In this work the only variable parameter is the overall molten salt content in the solution to be spun. Both Kelvin probe force microscopy (KPFM)<sup>13</sup> dedicated samples and LECs are prepared

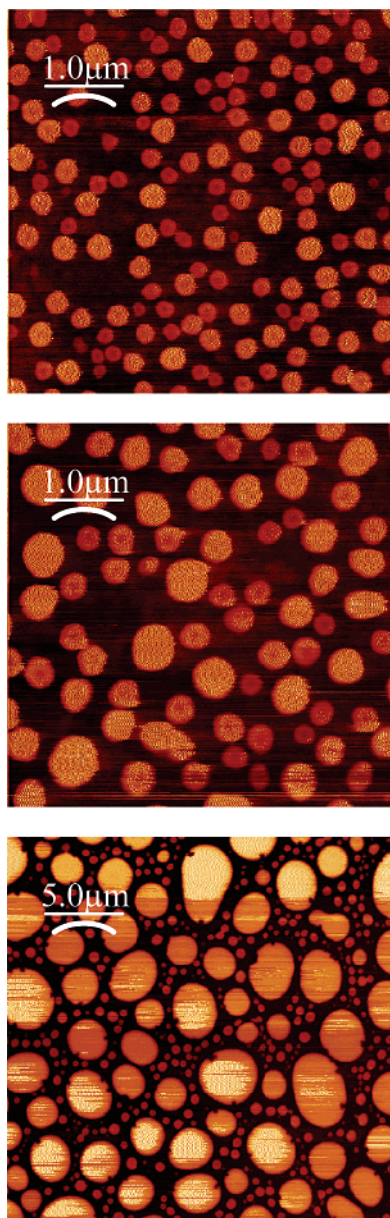


**Figure 2.** EFM images of three different polymer/molten salt blends with a polymer to salt concentration ratio given by 20–5 g/L, 20–12.5 g/L, and 20–30 g/L from the top to the bottom, respectively.

in a similar way. First we clean in acetone and propanol 1 cm<sup>2</sup> indium–tin-oxide (ITO)/glass substrates. We deposit by spin coating a 100 nm thick PEDOT-PSS layer, subsequently annealed for 15 min at 150 °C. Then we form the active layer by spin coating a chloroform solution containing the polymer/molten salt blend. The polymer concentration is always equal to 20 g/L, and the molten salt concentration is varied from 2 to 15 g/L. For LEC fabrication an additional metal deposition step is aimed at forming an Al cathode on top of the active layer.

## Results and Discussion

EFM imaging of the spin-coated layers is achieved in the dynamic mode. After a topographic scan, the tip is removed around 50 nm far from the surface and a sinusoidal voltage is applied between the sample and the tip at a frequency close to the cantilever resonance, with an amplitude not exceeding a few volts. This is quite similar to the measurement mode usually applied in KPFM,<sup>12</sup> except that we do not seek to cancel the electric force by adjusting a constant bias offset. Since for such

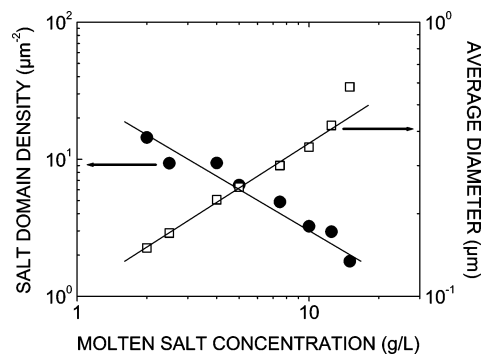


**Figure 3.** Average salt domain diameter and salt domain density versus molten salt concentration.

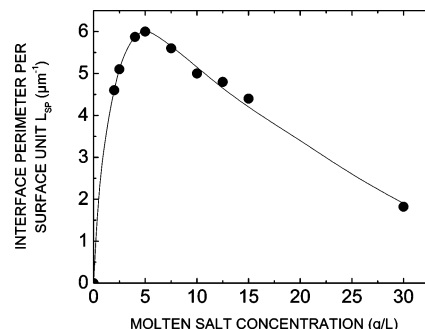


**Figure 4.** Interface perimeter per surface unit  $L_{SP}$  versus molten salt concentration, for a constant polymer concentration of 20 g/L. The solid line is a guide for the eyes.

electric fields the polymer is insulating and the salt is highly polarizable, this results in a high imaging contrast between the polymer and salt domains. In the dynamic mode this contrast is still higher than in the EFM static mode used in our previous report<sup>12</sup> (here we note that for our samples simple topographic AFM scans such as the ones successfully used in ref 14 are not sufficient to get a good contrast). In Figure 2, we show typical EFM images obtained for three different salt concentrations. Salt domains exhibit a discotic shape, and their density and size obviously vary with salt concentration in the solution. Since the LEC injection current is mainly favored in the polymer areas located close to a polarized salt domain, the current drive capability is expected to vary with the overall salt domain perimeter and thus to depend on two main factors: the salt domain density and diameter. From Figure 3 it can be seen that those two parameters exhibit qualitatively opposite trends with salt concentration. On one hand, the overall number of salt domains is almost inversely proportional to the molten salt concentration, and on the other hand, the average diameter of the salt domains increases with salt concentration roughly as a power law, at least for concentrations in a range extending from 1 to 10 g/L. For the largest concentrations the diameter distribution becomes bimodal, domains with a smaller diameter spreading around bigger salt domains (this self-organization process was already described in ref 12 and can be observed in the bottom image of Figure 2c). Those two competing trends (growing domain size and reduced density) result in the existence of an optimum concentration value, corresponding to a maximum in the average salt domain perimeter per unit area. This maximum is shown in Figure 4, in which the salt domain perimeter is plotted as a function of the salt content in the solution.

This particular dependence of the blend morphology on the overall molten salt content means that optimum conditions can be found for each specific salt–polymer couple. Since the

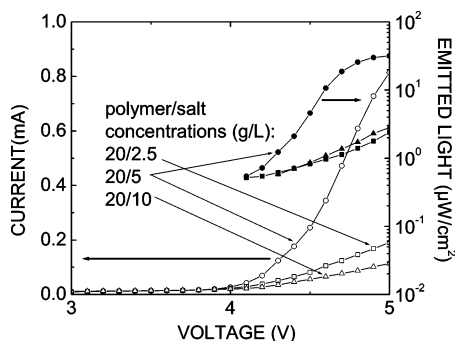


**Figure 5.** Current and emitted light versus voltage from three LECs processed with three different molten salt concentrations.

current usually increases with the salt domain perimeter,<sup>12</sup> we expect the best conditions for current drive capability to occur also at this maximum. To check this particular point we fabricated three runs of LECs with three different blends corresponding to polymer–salt concentration ratios equal to 20–5 g/L, 20–2.5 g/L, and 20–10 g/L, respectively. The first condition corresponds to the “optimum” blend defined by the maximum in Figure 4 and the two other values lie by each side of this maximum. Referring to Figure 4, we expect similar current levels for the 20–2.5 and 20–10 ratios since the salt domain interface length is in the same range for both values. Figure 5 shows typical current–voltage characteristics of LECs from the three variants. Current levels were quite reproducible from one device to another. From Figure 5 it is clear that the LEC fabricated from the blend with the 20–5 g/L ratio exhibits a much higher current than its two other counterparts, with a factor of improvement larger than 4. This difference is still enhanced for electroluminescence (EL), for which the improvement factor is around 10 (Figure 5). This result confirms both that carrier injection preferentially occurs in the polymer areas closest to the salt domains, and that there is an optimum salt content value, which corresponds to a molten salt–polymer blend with a maximized interface length between both kinds of domains. Additionally, the threshold voltage does not change with the salt content, which is a further indication that the only modification brought by a variation in salt content is a change in the effective area over which current is injected.

## Conclusion

This work has highlighted the importance of finding optimized conditions to produce the molten salt–polymer blends best suited for favoring electron and hole injection in thin layer electrochemical cells. By means of EFM measurements, we showed that increasing the salt content results in producing a reduced number of larger salt domains, so that the overall perimeter of the discotic salt domains exhibits a maximum as a function of the salt concentration in the solution. We checked that this maximum does lead to a maximum in current drive capability and EL intensity, so that its position should be precisely determined for each particular couple of molten salt and conjugated polymer. EFM/AFM observation thus reveals to be an invaluable tool for optimizing the blend.

**Acknowledgment.** We thank J. Chevrier (CNRS/LEPES and European Synchrotron Radiation Facility, Grenoble) for letting the AFM equipment at our disposal to characterize the polymer/molten salt blends.

## References and Notes

- (1) Seki, S.; Kobayashi, Y.; Miyashiro, H.; Ohno, Y.; Usami, A.; Mita, Y.; Kihira, N.; Watanabe, M.; Terada, N. *J. Phys. Chem. B* **2006**, *110*, 10228.
- (2) Panozzo, S.; Armand, M.; Stéphan, O. *Appl. Phys. Lett.* **2002**, *80*, 679.
- (3) Ouisse, T.; Armand, M.; Kervella, Y.; Stéphan, O. *Appl. Phys. Lett.* **2002**, *81*, 3131.
- (4) Ouisse, T.; Stéphan, O.; Armand, M.; Leprêtre, J. C. *J. Appl. Phys.* **2002**, *92*, 2795.
- (5) Pei, Q.; Yu, G.; Zhang, C.; Heeger, A. J. *Science* **1995**, *269*, 1086.
- (6) Pei, Q.; Yang, Y.; Yu, G.; Zhang, C.; Heeger, A. J. *J. Am. Chem. Soc.* **1996**, *118*, 3922.
- (7) Yang, Y.; Pei, Q. *J. Appl. Phys.* **1997**, *81*, 3294.
- (8) Yang, C.; Sun, Q.; Qiao, J.; Li, Y. *J. Phys. Chem. B* **2003**, *107*, 12981.
- (9) Edman, L. *Electrochim. Acta* **2005**, *50*, 3878.
- (10) Hu, Y.; Tracy, C.; Gao, J. *Appl. Phys. Lett.* **2006**, *88*, 123507.
- (11) Li, Y.; Cao, Y.; Gao, J.; Wang, D.; Yu, G.; Heeger, A. J. *Synth. Met.* **1999**, *99*, 243.
- (12) Habrard, F.; Ouisse, T.; Stéphan, O.; Armand, M. *J. Appl. Phys.* **2004**, *96*, 7219.
- (13) Jacobs, H. O.; Leuchtmann, P.; Homan, O. J.; Stemmer, A. *J. Appl. Phys.* **1998**, *84*, 1168.
- (14) Wenzl, F. P.; Suess, C.; Haase, A.; Poelt, P.; Somitsch, D.; Knoll, P.; Scherf, U.; Leising, G. *Thin Solid Films* **2003**, *433*, 263.